Journal of Hepatocellular Carcinoma

Dovepress
Taylor & Francis Group

Open Access Full Text Article

ORIGINAL RESEARCH

Hypoxia- and Anoikis-Related lncRNA Signature Defines Molecular Subtypes and Predicts Prognosis and Immunotherapy Response in Hepatocellular Carcinoma

Xiaohang Lu[1–3,*], Yunyong Wang[1,3,*], Yuan Yu[4], Rongzhen Zhang[5], Fuli Long[5], Minpeng Li[4], Meng Pan[4], Kewei Du[6], Jinna Tan[1,3], Jiaqian He[1,3], Zongxian Li[7,8], Hongsheng Lin[1,6,*], Mingfen Li[1,6,*]

[1]The First Affiliated Hospital of Guangxi University of Chinese Medicine, Nanning, 530023, People's Republic of China; [2]Department of Ophthalmology, The People's Hospital of Guangxi Zhuang Autonomous Region, Nanning, 530016, People's Republic of China; [3]Guangxi Key Laboratory of Molecular Biology of Preventive Medicine of Traditional Chinese Medicine, Nanning, 530023, People's Republic of China; [4]Hepatobiliary Surgery, The First Affiliated Hospital of Guangxi University of Chinese Medicine, Nanning, 530023, People's Republic of China; [5]Department of Hepatology, The First Affiliated Hospital of Guangxi University of Chinese Medicine, Nanning, 530023, People's Republic of China; [6]Laboratory Department, The First Affiliated Hospital of Guangxi University of Chinese Medicine, Nanning, 530023, People's Republic of China; [7]Department of Clinical Laboratory, The First Affiliated Hospital of Guangxi Medical University, Nanning, 530020, People's Republic of China; [8]Key Laboratory of Clinical Laboratory Medicine of Guangxi Department of Education, Nanning, 530020, People's Republic of China

*These authors contributed equally to this work

Correspondence: Mingfen Li; Hongsheng Lin, Laboratory Department, The First Affiliated Hospital of Guangxi University of Chinese Medicine, No. 89-9 Dongge Road, Qingxiu District, Nanning, Guangxi Zhuang Autonomous Region, People's Republic of China, Email limf@gxtcmu.edu.cn; linhs@gxtcmu.edu.cn

Background: Hepatocellular carcinoma (HCC) is characterized by high incidence and mortality rates, with hypoxia and anoikis resistance playing crucial roles in its progression and metastasis. While long non-coding RNA (lncRNA) significantly influence tumor biology, their roles in hypoxia-anoikis-resistant HCC remain unclear.

Methods: This study utilized RNA-seq data and clinical information from the TCGA and GEO databases to analyze 154 hypoxia- and anoikis-related lncRNAs and identify differentially expressed candidates. Cluster analysis with Consensus Cluster Plus revealed links to clinical outcomes and genomic features. Tumor immune microenvironment and pathway enrichment were assessed using CIBERSORT and ssGSEA. A nine-gene risk model was developed via LASSO Cox regression and internally validated. Preliminary experimental assays suggested that the identified lncRNAs may influence apoptosis under hypoxia and anoikis conditions.

Results: HCC patients were classified into two molecular subtypes, C1 and C2, with distinct prognostic outcomes and clinical features. These subtypes showed distinct immune infiltration characteristics and differential immunotherapy response scores. A nine-lncRNA prognostic model effectively predicted overall survival (OS), with the high-risk group showing increased immunosuppressive elements, such as Tregs and inactivated M0 macrophages, suggesting limited immunotherapy efficacy. Chemotherapy sensitivity analysis revealed varying drug responses between risk groups, while hypoxia- and anoikis-related lncRNAs, including *LINC01554*, *FIRRE*, *LINC01139*, *LINC01134* and *NBAT1* were downregulated in this model.

Conclusion: Research has demonstrated that hypoxia- and anoikis-related lncRNAs serve as reliable biomarkers for predicting liver cancer prognosis and immunotherapy response, offering potential for developing novel therapeutic targets and strategies to enhance treatment outcomes and patient prognosis.

Keywords: hepatocellular carcinoma, anoikis, hypoxia, LncRNA, molecular subtypes

Introduction

Hepatocellular carcinoma (HCC) ranked as the third leading cause of cancer mortality globally in 2020, accounting for 75%-85% of primary liver cancers.[1] Treatment modalities for HCC encompass surgical resection, chemotherapy, transcatheter

Received: 7 April 2025
Accepted: 15 August 2025
Published: 13 October 2025

arterial chemoembolization (TACE), and systemic therapy. However, most HCC cases are diagnosed at advanced stages, missing the optimal window for surgical intervention. Even post-resection, HCC exhibits alarming 5-year recurrence rates ranging between 60%-70%.[2] Metastasis and relapse are primary factors that significantly impact patients' long-term survival, posing a critical challenge in the overall management of HCC.[3] In recent years, traditional Chinese medicine (TCM) has gained attention as a complementary approach in HCC treatment due to its multi-targeted mechanisms, including modulation of tumor growth, metastasis, and immune responses, which may improve therapeutic efficacy and reduce adverse effects.[4] Therefore, a comprehensive understanding of the molecular mechanisms orchestrating the metastatic cascade is crucial for advancing HCC treatment, potentially revealing new therapeutic targets and integrative strategies.

Tumor metastasis remains the leading cause of cancer-related mortality worldwide.[5] During this complex process, tumor cells must detach from the primary lesion, degrade the extracellular matrix (ECM), intravasate into the bloodstream, survive circulatory stress, extravasate, and ultimately colonize distant organs.[6] Among the many factors influencing this metastatic cascade, anoikis resistance and hypoxia are two critical stress responses that significantly contribute to tumor progression.[7,8] Anoikis, or anchorage-dependent programmed cell death, is typically induced when epithelial cells lose contact with the ECM.[7] However, epithelial-derived tumor cells frequently acquire anoikis resistance during malignant transformation, particularly in metastatic settings, which enables them to survive in suspension, traverse the vasculature, and establish metastases.[9] HCC, which arises from epithelial hepatocytes and exhibits strong vascularity, often displays features of anoikis resistance, facilitating hematogenous dissemination.[10] In parallel, hypoxia is a hallmark of the solid tumor microenvironment (TME) and plays a pivotal role in promoting tumor aggressiveness. HCC frequently experiences intratumoral hypoxia due to rapid proliferation and abnormal vasculature.[11] Hypoxia not only enhances invasion and migration but also sustains cancer stemness through the activation of oncogenic pathways such as Wnt/β-catenin.[12] Furthermore, hypoxia profoundly reshapes the tumor immune microenvironment (TIME) by modulating immune cell infiltration, inducing immunosuppressive phenotypes, and promoting immune evasion, which collectively facilitate tumor progression and metastasis.[13] Although both hypoxia and anoikis resistance are critical in HCC progression, they are often studied separately, with limited focus on their combined effects.

Long non-coding RNA (lncRNA), a class of transcripts longer than 200 nucleotides, have emerged as important regulators of tumor biology, including proliferation, metastasis, recurrence, prognosis, and therapeutic response.[14–17] LncRNAs can be functionally categorized into immune-related, hypoxia-responsive, EMT-related, and anoikis-associated types.[18–21] For instance, hypoxia-responsive lncRNAs such as *LINC00839* are transcriptionally activated under oxygen-deprived conditions and modulate tumor proliferation and immune evasion.[18] Likewise, anoikis-related lncRNAs such as *AL031985.3* and *AC026412.3* promote anchorage-independent survival and enhance metastatic potential.[21] Although both hypoxia- and anoikis-related lncRNAs have been individually studied in HCC, integrated analyses remain scarce. To the best of our knowledge, no prior studies have systematically combined hypoxia- and anoikis-related lncRNA signatures to define molecular subtypes or predict immune landscape and prognosis in HCC. Given the converging effects of these stress responses on tumor stemness, immune suppression, and metastasis, their integration may yield a more comprehensive understanding of tumor biology and guide treatment stratification.

In this investigation, hypoxia- and anoikis-related lncRNAs were identified, and gene expression datasets and clinical data of liver cancer patients were retrieved from TCGA GDC API and GSE43619 databases. The study aimed to explore the interplay between hypoxia- and anoikis-related lncRNAs and the prognosis of HCC patients. By utilizing hypoxia- and anoikis-related lncRNAs, HCC was stratified into two molecular subtypes, with comparative evaluations of immunophenotypic characteristics across these subsets. Furthermore, a prognostic model centered around hypoxia- and anoikis-related lncRNAs was developed to decipher their associations with HCC prognosis and tumor immunophenotype (Figure 1). This research effort contributes to understanding the implications of hypoxia- and anoikis-related lncRNAs in HCC, unveiling new avenues for metastasis biomarkers and clinical interventions.

Materials and Methods

Data Sources

RNA-seq data from TCGA GDC API (https://gdc.cancer.gov/developers/gdc-application-programming-interface-api) were utilized to download expression data and clinical follow-up information of LIHC samples. The RNA-Seq data

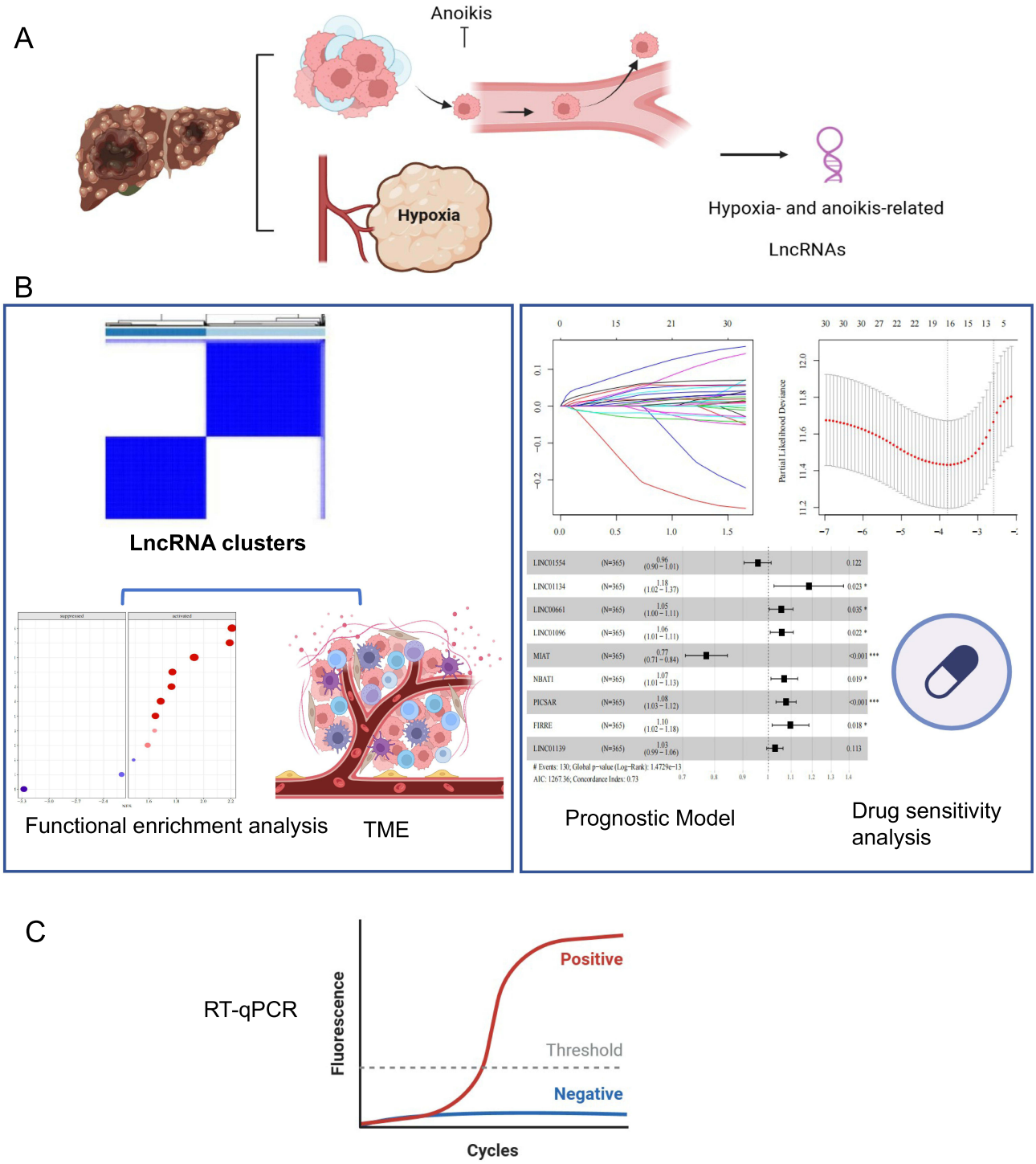

Figure 1 Research process. (**A**) Identification of Hypoxia- and anoikis-related lncRNA genes. (**B**) Construction and validation of gene prognostic model. (**C**) Experimental verification.

from TCGA-LIHC removed samples without survival time and status, converted Ensembl to Gene symbol, transformed the expression matrix into TPM format, and performed log2 conversion. The TCGA-LIHC cohort was used for the construction and internal validation of the risk model. Additionally, gene expression data and clinical information from the GSE188608 and GSE103581 cohorts were downloaded from the Gene Expression Omnibus (GEO) database (https://www.ncbi.nlm.nih.gov/geo/). These datasets were specifically used to identify hypoxia- and anoikis-related lncRNAs.

The GSE43619 dataset was also obtained from GEO and used for external validation of the constructed prognostic model. Platform-specific annotation files were used to map probe IDs to gene symbols, and the average expression value was taken when multiple probes corresponded to a single gene. Subsequently, 365 HCC samples and 50 adjacent control samples were acquired. For the GSE43619 data, the annotation information of the corresponding chip platform was downloaded, and probes were mapped to genes where the mean value was considered as the gene expression. This research utilized secondary datasets that had been fully de-identified and contained no personally identifiable information; therefore, ethical approval was not required. As the data originated from publicly accessible genomic databases and the study did not involve any direct contact with human subjects or implementation of invasive procedures, informed consent was waived. In accordance with relevant ethical guidelines on the use of public data, this study meets the criteria for exemption from both ethical review and informed consent requirements.

Differential lncRNA Identification and Risk Model Construction

Utilizing the ConsensusClusterPlus package, a consistency matrix was constructed through consistency clustering, and the samples were classified based on specific parameters. The clustering algorithm was set to "km" with a distance of "euclidean". The process was repeated 500 times with an 80% sampling ratio each time to ensure clustering reliability. For ConsensusClusterPlus analysis, the optimal number of clusters (k) was selected based on the cumulative distribution function (CDF) curve and delta area plot. The most stable clustering was observed when $k = 2$.

Differential lncRNA Identification

Differential analysis between C1 and C2 subtypes was conducted using the limma package with an FDR threshold of 0.05. Subsequently, the survival R package was employed to perform univariate Cox proportional hazard regression on the differential genes, considering a significance level of $p < 0.05$. For LASSO-Cox regression, the lambda parameter was determined using 10-fold cross-validation to minimize partial likelihood deviance, and the value of lambda.min was selected. Stepwise multivariate regression analysis further reduced the gene set.

Prognostic Model Construction and Validation

LASSO Cox regression analysis was utilized to reduce the number of genes with key genes and correlation coefficients determined through stepwise regression. The risk score for each patient was calculated using a specific formula. The optimal threshold for dividing high and low-risk groups was determined using the survminer package. Kaplan-Meier and ROC analyses were performed to evaluate the prognostic classification of RiskScore using the R software package timeROC.

Immune Infiltration and Therapy Response Prediction

Various packages like GSVA, ESTIMATE, CIBERSORT, TIDE, and pRRophetic were utilized for immune infiltration evaluation and immunotherapy prediction.[22] The Immunophenoscore (IPS) was calculated, and the sensitivity of chemotherapy drugs was predicted.

Gene Set Enrichment Analysis (GSEA)

GSEA was employed to analyze different biological processes across molecular subtypes using the HALLMARK pathway gene set downloaded from the molecular feature database (https://www.gseamsigdb.org/gsea/msigdb/).

Cell Culture and Real-Time Fluorescence Quantitative PCR (RT-qPCR)

Human HCC cell line Li-7 (RRID:CVCL_3840) was provided by the stem cell bank of the Chinese Academy of Sciences. Cells were cultured in 1640 (Gibco, USA) medium containing 10% fetal bovine serum at 37 °C and 5% CO_2. The number of 1×10^6 cells was placed in an ultra-low adsorption 6-well plate and cultured for 24 h under hypoxia conditions containing 1% O_2, 5% CO_2, and 37 °C. All experiments were divided into 3 replicates. Total RNA was extracted using RNeasy Mini Kit (Magen, China) and cDNA was synthesized using PrimeScript TM RT Master Mix (Takara, China). The primers were designed and synthesized by servicebio. RT-qPCR was performed using TB Green®

Premix Ex Taq TM II and LightCycler 480 System. The results show that it is $2^{-\Delta\Delta Ct}$. The mRNA expression of 5 lncRNAs was randomly detected, and GAPDH was selected as the internal reference gene. All experiments were divided into 3 replicates. The primer sequence is detailed in Table 1.

Western Blotting

The cells in the six-well plate were lysed using RIPA lysis buffer and protease inhibitor (PMSF) to extract total protein. The lysed cells were centrifuged at 14,000 rpm for 15 min and the supernatant containing the total protein was quantified by the BCA protein assay kit (Beyotime, Shanghai, China). The 30 μg protein was used for 12% SDS-PAGE electrophoresis to separate the protein, and then the protein was transferred to the PVDF membrane. After blocking with 5% skim milk for 1 h, the membrane was incubated with the primary antibody at 4 °C overnight. After washing with TBST buffer, the second antibody coupled with horseradish peroxidase was added to the membrane and incubated for 40 min. The protein bands were displayed using ECL reagents and analyzed using ImageJ software. The antibodies were as followed: β-actin (Santa Cruz Biotechnology, 1:1000), HIF-1α (Cell Signaling Technology, 1:1000).

Short Interfering RNA (siRNA) Transfection

Li-7 cells were transiently transfected with target-specific siRNA or negative control siRNA (siNC). All individual siRNAs were designed and synthesized by Sangon Biotech. The cells were cultured in six-well plates until they reached 60–70% confluence and then transfected using RNA TransMate reagent (Sangon Biotech). Cells were harvested 48 h post-transfection. The sequence information of siRNA is shown in Table 2.

Flow CytoMetry

Apoptosis was assessed using the Annexin V-APC/DAPI Apoptosis Kit (Elabscience®, Wuhan, China). The cell quantity and culture conditions are as described in Cell Culture. Harvest the cells and centrifuge at 300 ×g for 5 min. Remove the supernatant, wash the cells once with PBS, and centrifuge again to discard the wash buffer. Resuspend the cells in 100 μL of diluted 1× Annexin V Binding Buffer. Add 2.5 μL of Annexin V-APC Reagent and 2.5 μL of DAPI Reagent (25 μg/mL). Mix thoroughly and incubate at room temperature in the dark for 15 min. Finally, add 400 μL of diluted 1× Annexin V Binding Buffer, mix gently, and analyze the samples using flow cytometry.

Table 1 Primers Used for RT-qPCR

Gene	Sequence 5'→3'	
GAPDH	Forward Primer Reverse primer	CAAATTCCATGGCACCGTCA GACTCCACGACGTACTCAGC
LINC01554	Forward primer Reverse primer	GACGAGGGCCTTTGTCAGAA TCTGCCTGTAAATGCCCCAG
FIRRE	Forward primer Reverse primer	TGCAGCTAGGAGGACCTTGA TAATGCCACCTCCAGCAGAC
LINC01139	Forward primer Reverse primer	TGACTGATGCTTCCCCAAAAC CCTCCCACCTGGCTGTCTTA
LINC01134	Forward primer Reverse primer	GCCACCCTGGACTCCTAAAC GCGGACAGAAATCCCCTTGA
NBAT1	Forward primer Reverse primer	GCCTGGGTCATCTCACAGAG ACAGGGCCCTATCCTATGGT

https://doi.org/10.2147/JHC.S521878

Table 2 The Sequence Information of siRNA

Gene	Sequence 5'→3'	
LINC01554	Sense Antisense	GUGUAGAAAUUCAAAUGAA/dT//dT/ UUCAUUUGAAUUUCUACAC/dT//dT/
LINC01139	Sense Antisense	GGUAUGAAAUUGUUGUGUA/dT//dT/ UACACAACAAUUUCAUACC/dT//dT/

Abbreviations: HCC, Hepatocellular carcinoma; LncRNA, Long non-coding RNA; TACE, transcatheter arterial chemoembolization; ECM, Extracellular matrix; TME, Tumor microenvironments; GEO, Gene Expression Omnibus; IPS, Immune Profiling System; TIDE, Tumor Immune Dysfunction and Exclusion; MDSC, Myeloid-derived suppressor cells; ssGSEA, Single-sample Gene Set Enrichment Analysis; AFP, Alpha-fetoprotein; EMT, Epithelial-Mesenchymal Transition; EGFR, Epidermal growth factor receptor; ICI, Immune checkpoint inhibitors; CRC, Colorectal cancer; RT-qPCR, Real-time fluorescence quantitative PCR.

Statistical Analysis

All statistical data were analyzed using R language (version 3.6.0). Continuous variables such as gene expression, immune scores, and pathway enrichment levels were compared using the Wilcoxon rank-sum test. Differences in categorical clinical characteristics between groups were evaluated using the chi-square test. Spearman correlation analysis was employed to assess associations between risk scores and immune infiltration or pathway activity. RT-qPCR and flow cytometry data are presented as mean ± standard deviation, and comparisons among multiple groups were conducted using one-way analysis of variance (ANOVA). All tests were two-sided, and a $p < 0.05$ was considered statistically significant.

Results

Identification of Prognostic Hypoxia- and Anoikis-Related lncRNAs and Classification of HCC Molecular Subtypes

To explore the role of hypoxia- and anoikis-related lncRNAs in HCC, we integrated data from the GSE103581 and GSE188608 datasets, identifying 154 lncRNAs significantly associated with overall survival in the TCGA-LIHC cohort ($p < 0.05$; Supplementary Table 1). Among them, 61 lncRNAs were differentially expressed between tumor and adjacent normal tissues (Supplementary Figure 1A), and 49 were further validated to be prognostically relevant (lncRNA_cox.csv). The intersection of these datasets yielded 25 lncRNAs (Supplementary Figure 1B), among which *LINC01018* and *LINC01554* were more highly expressed in normal tissues, while the remaining lncRNAs were upregulated in tumor samples (Supplementary Figure 1C).

Based on the expression profiles of these 25 lncRNAs, consensus clustering analysis was performed using the TCGA-LIHC dataset. Two robust molecular subtypes, C1 and C2, were identified (Figure 2A and B). Survival analysis revealed a significantly worse prognosis in the C1 subtype compared to C2 (Figure 2C). Further characterization using the six established immune subtypes (C1–C6) demonstrated that the majority of HCC samples in both molecular subtypes corresponded to immune subtypes C3 (inflammatory) and C4 (lymphocyte-depleted), with minimal overlap with C5 (immunologically quiet) and C6 (TGF-β dominant) (Figure 2D). Notably, C2 contained a higher proportion of patients with aggressive immune subtypes (C1 and C2), consistent with its poorer immune-associated survival outcomes (Figure 2E). These findings highlight the potential of hypoxia- and anoikis-related lncRNAs not only as prognostic markers but also as classifiers of HCC molecular subtypes with distinct immune landscapes and clinical outcomes.

Integrated Genomic and Immunological Characterization of C1 and C2 Subtypes Reveals Distinct Tumor Biology and Immunotherapy Responses

To further elucidate the biological differences between the C1 and C2 subtypes, we investigated their genomic alterations, somatic mutations, immune microenvironment profiles, and pathway enrichment.[23] Genomic instability was more pronounced in the C1 subtype, which exhibited significantly higher levels of fraction genome altered, number

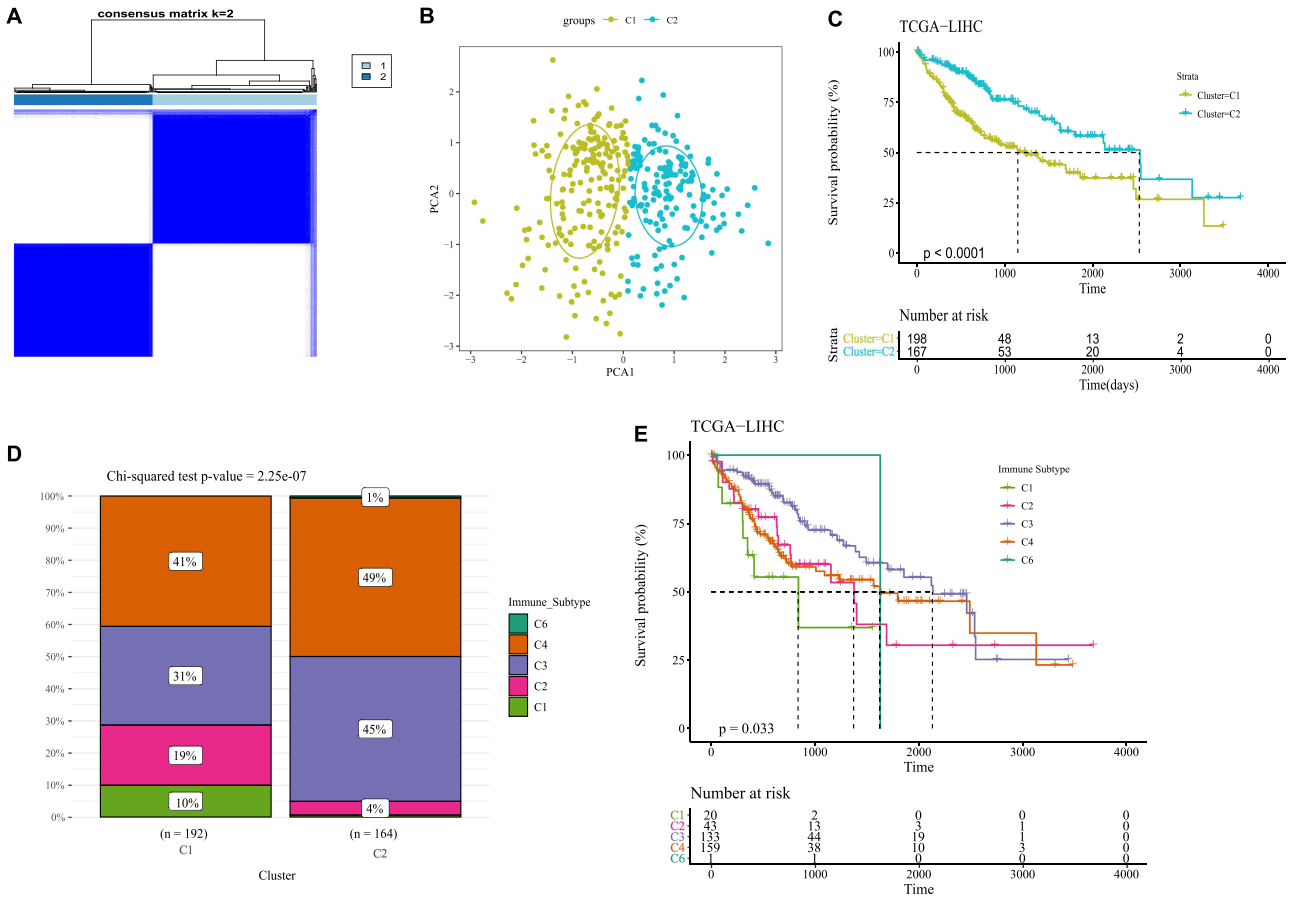

Figure 2 Molecular subtype construction and prognosis analysis. (**A**) TCGA-LIHC sample clustering heat map. (**B**) PCA of TCGA molecular subtypes. (**C**) Survival analysis between TCGA subtypes. (**D**) Comparison of the distribution of immune subtypes between different molecular subtypes. (**E**) Survival curve of immune subtypes.

of segments, and homologous recombination deficiency scores (Figure 3A). Fisher's exact test identified subtype-specific somatic mutations ($p < 0.01$), revealing that C1 had higher mutation frequencies in TP53, DMD, TG, and GREB1, whereas C2 was enriched for mutations in BIRC6, DOCK8, HERC1, IL6ST, CREBBP, and OR2J3 (Figure 3B and C).

We next examined the immune landscape of these subtypes. ESTIMATE analysis showed that the C1 subtype had elevated stromal and immune scores, indicating increased immune and matrix component infiltration (Figure 4A). CIBERSORT analysis revealed that C1 harbored higher proportions of immunosuppressive cells, including regulatory T cells (Tregs), M0 macrophages, and memory B cells (Figure 4B). In contrast, single-sample GSEA (ssGSEA) demonstrated overall enhanced immune activation in C1, including increased infiltration of CD4+ and CD8+ T cells, B cells, NK cells, dendritic cells, and macrophages. Despite this heightened immune cell presence, the elevated myeloid-derived suppressor cell (MDSC) score in C1 suggests a coexisting immunosuppressive milieu, potentially contributing to immune evasion. Meanwhile, C2 showed modest immune activity with relatively higher scores for activated dendritic cells (Figure 4C). Integrative comparison with immune-related genomic signatures reported in HCC literature indicated that the C1 subtype scored significantly higher in proliferation, TGF-β response, and aneuploidy, supporting a more aggressive and genomically unstable phenotype (Figure 4D). Immunotherapy sensitivity prediction revealed higher Immunophenoscore (IPS) and lower TIDE scores in the C2 subtype, suggesting greater potential responsiveness to immune checkpoint blockade in these patients (Figure 4D). Finally, we compared the differences in activation pathways between C1 and C2 subtypes. GSEA pathway analysis showed that C1 was enriched in oncogenic and EMT-related pathways, including E2F targets, G2M checkpoint, and epithelial-mesenchymal transition, while C2 was associated with metabolic pathways, particularly bile acid metabolism (Figure 4E).

https://doi.org/10.2147/JHC.S521878

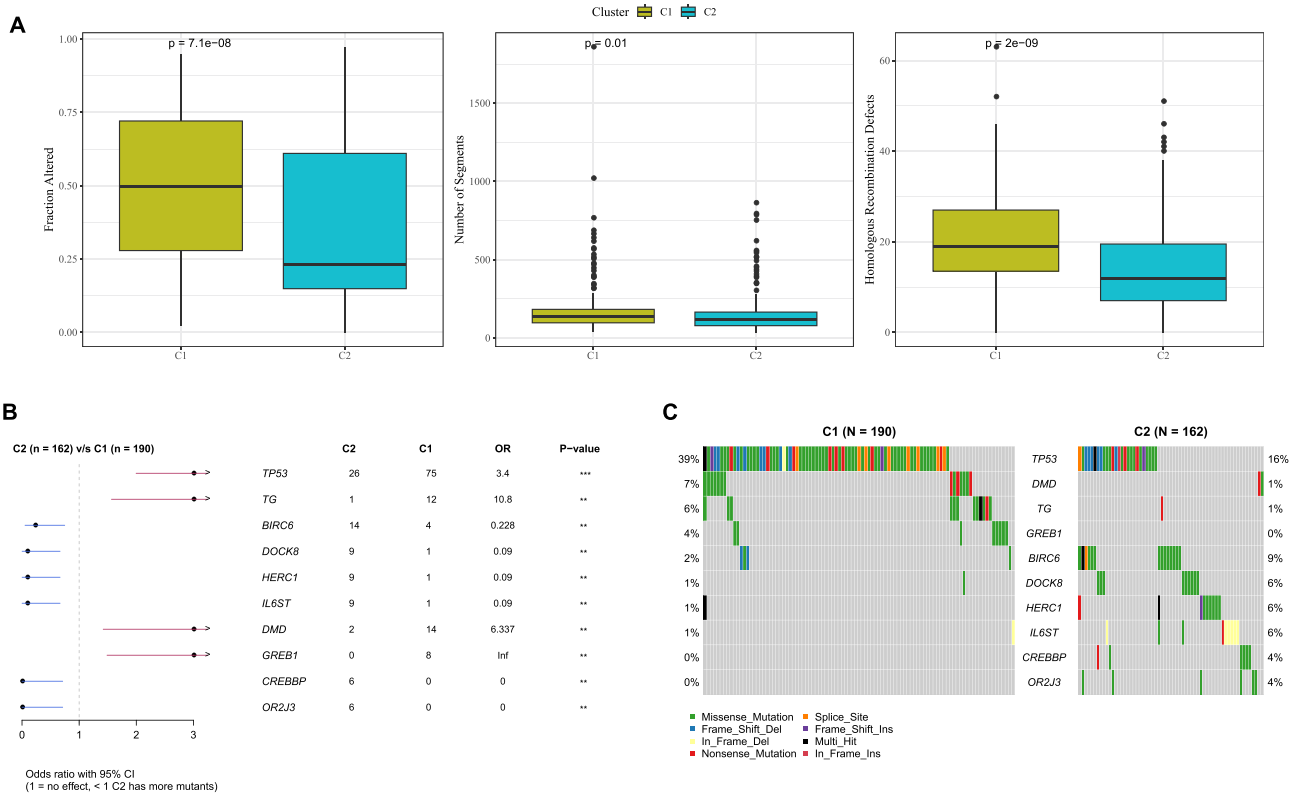

Figure 3 Genomic characteristics and somatic mutations among different subtypes. (**A**) Genome feature score between C1 and C2 subtypes. (**B** and **C**) Forest map and waterfall map of differential mutation genes between C1 and C2 subtypes.
Notes: (C) X-axis shows gene names. Each cell shows mutation frequency (%), with colors or symbols representing mutation types.

Construction and Validation of a Prognostic 9-lncRNA Risk Model

A total of 61 differentially expressed lncRNAs were identified between the C1 and C2 subtypes (Figure 5A). These candidates were first subjected to univariate Cox regression to screen for prognosis-related genes, followed by LASSO Cox regression to reduce overfitting and refine the model (Figure 5B and C). Subsequently, stepwise multivariate Cox regression further narrowed the list, and nine lncRNAs were ultimately identified as independent prognostic factors: *LINC01554*, *LINC01134*, *LINC00661*, *LINC01096*, *MIAT*, *NBAT1*, *PICSAR*, *FIRRE*, and *LINC01139* (Figure 5D). The final risk model was constructed based on their expression and corresponding coefficients as follows: Risk score = (−0.044 * LINC01554) + (0.168 * LINC01134) + (0.053 * LINC00661) + (0.056 * LINC01096) + (−0.258 * MIAT) + (0.067 * NBAT1) + (0.074 * PICSAR) + (0.093 * FIRRE) + (0.028 * LINC01139).

Based on this formula, risk scores were calculated for each patient, and individuals were stratified into high- and low-risk groups. Kaplan-Meier survival analysis revealed that patients in the high-risk group had significantly worse overall survival than those in the low-risk group (Figure 6A). The model also showed strong predictive accuracy, with a high area under the ROC curve (AUC) (Figure 6B). Expression profiling demonstrated that *LINC01554* and *MIAT* were predominantly expressed in the low-risk group, whereas the other seven lncRNAs were significantly upregulated in the high-risk group (Figure 6C). The prognostic value of this model was further validated in the independent GSE43619 cohort, with similar survival stratification and predictive performance (Figure 6D–F).

Multi-Dimensional Evaluation of the 9-lncRNA Risk Model: Prognostic Value, Immune Infiltration, and Drug Response

To evaluate the clinical relevance of the 9-lncRNA-based risk score, we compared the clinicopathological features between high- and low-risk groups in the TCGA cohort. As tumor grade and AJCC stage increased, the corresponding

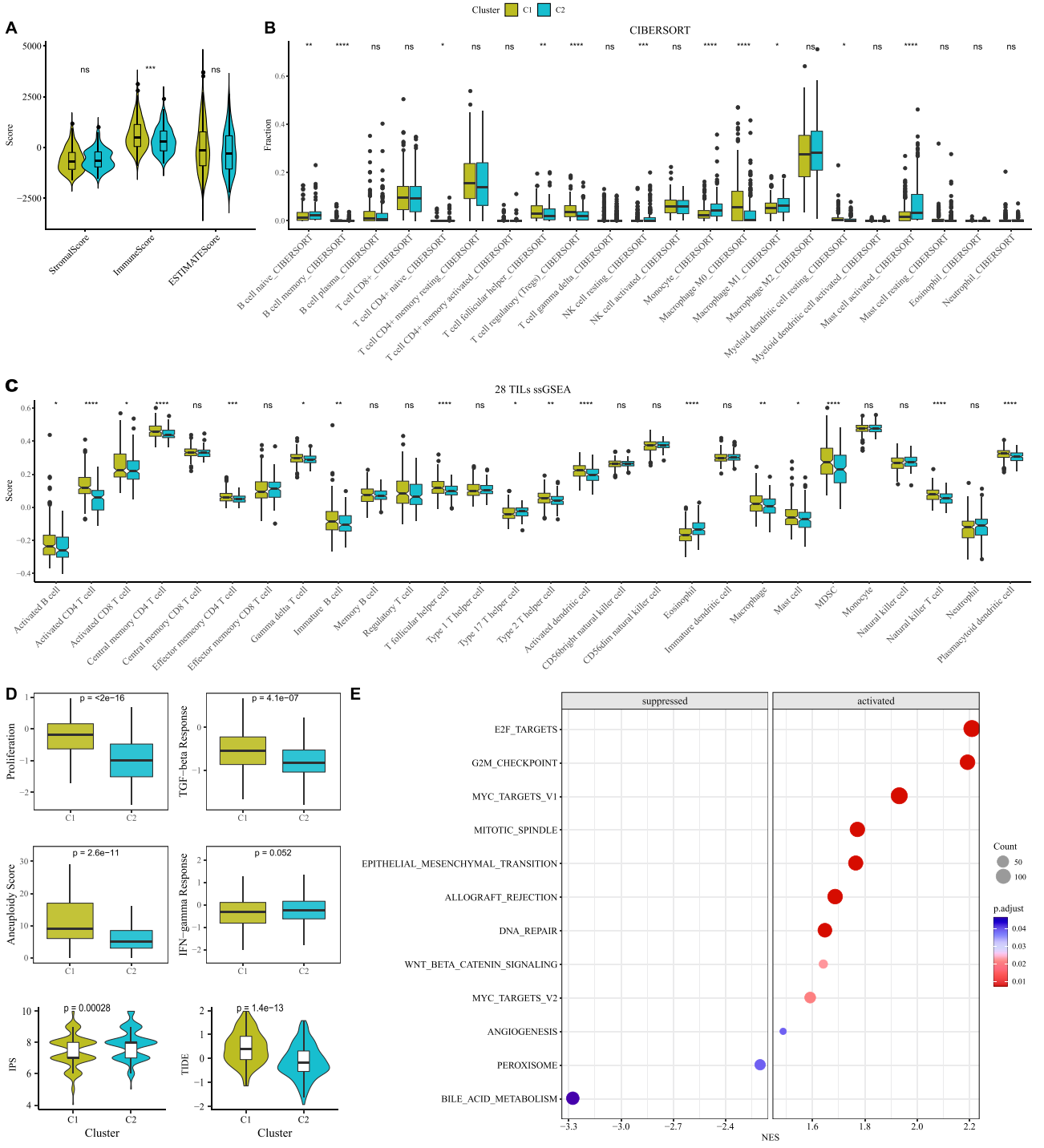

Figure 4 Analysis of immune microenvironment of two subtypes. (**A**) ESTIMATE immune score difference between subtypes. (**B**) CIBERSORT immune infiltration difference between subtypes. (**C**) 28 immune score differences between subtypes. (**D**) Proliferation, TGF-beta Response, Aneuploidy score, and immunotherapy sensitivity comparison between subtypes. (**E**) Differences in pathway activity between subtypes.
Notes: *p < 0.05, **p < 0.01, ***p < 0.001, ****p < 0.0001.

risk score also significantly increased, indicating a strong association between molecular risk and disease severity (Figure 7A). Univariate and multivariate Cox regression analyses identified both RiskScore and AJCC stage as independent prognostic factors for overall survival (Figure 7B and C). A combined nomogram integrating RiskScore and AJCC stage demonstrated that RiskScore had the greatest impact on survival prediction (Figure 7D). The calibration

https://doi.org/10.2147/JHC.S521878

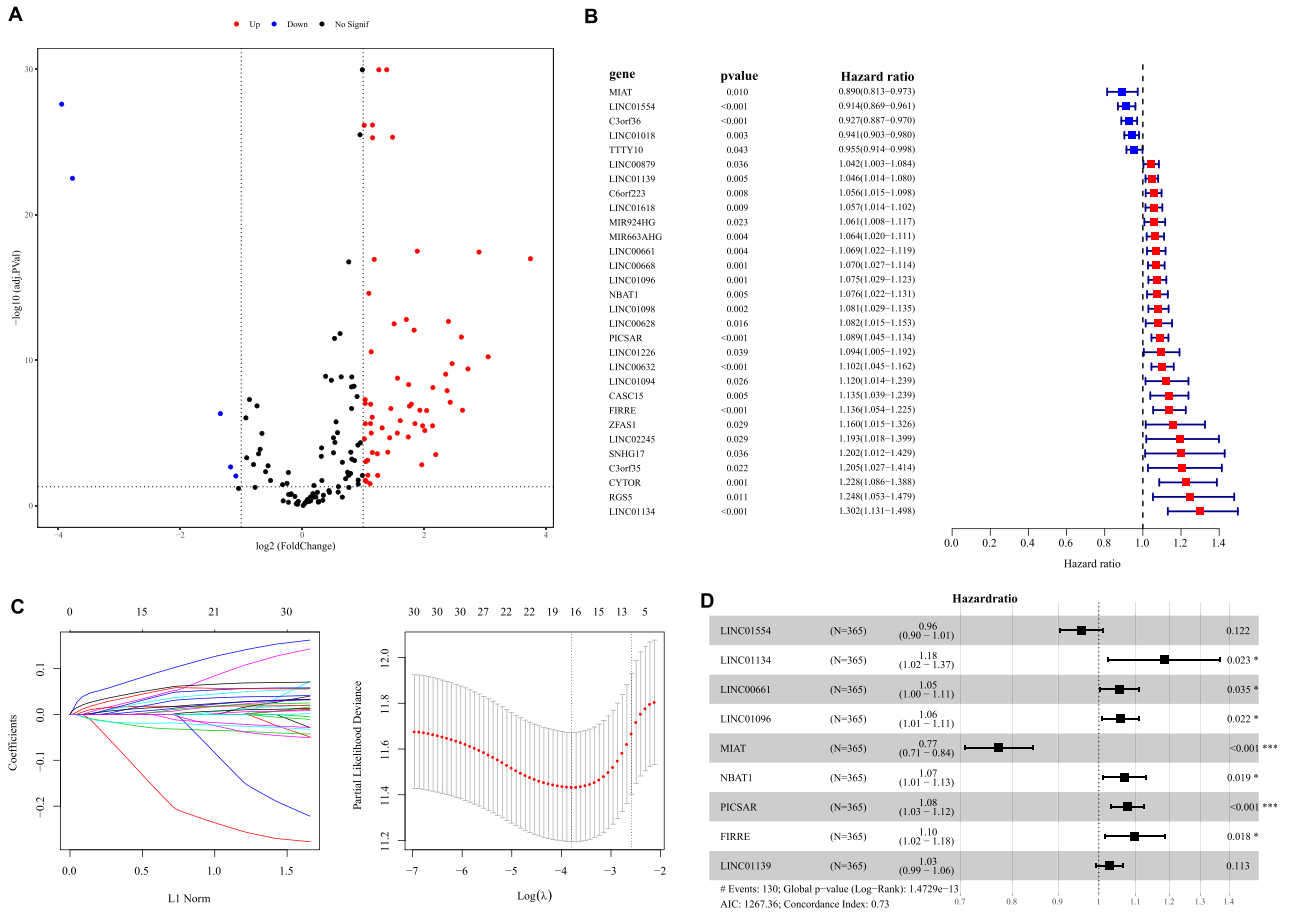

Figure 5 Nine lncRNAs were identified as key genes affecting prognosis. (**A**) Differential lncRNA identification between C1 and C2 subtypes in TCGA. (**B**) Differential lncRNA prognostic forest map. (**C**) LASSO narrows the gene range. (**D**) Multi-factor forest map of characteristic genes.
Note: The volcano map threshold is adj.p <0.05 and |log2FC|> 1.

curve showed strong agreement between predicted and observed survival at 1, 3, and 5 years (Figure 7E), and decision curve analysis (DCA) confirmed that the nomogram and RiskScore provided greater net clinical benefit than traditional clinical indicators (Figure 7F).

To explore immune landscape differences between risk groups, we used ESTIMATE and found that the low-risk group had significantly higher StromalScore, ImmuneScore, and ESTIMATEScore, along with lower tumor purity, suggesting a more active immune microenvironment (Figure 8A and B). Further correlation analysis using CIBERSORT indicated that RiskScore was negatively associated with $CD8^+$ T cells and M1 macrophages, but positively correlated with immunosuppressive cells such as Tregs and M0 macrophages (Figure 8C). Moreover, the low-risk group exhibited higher Immunophenoscore (IPS) and lower Tumor Immune Dysfunction and Exclusion (TIDE) scores, suggesting a greater potential for response to immunotherapy (Figure 8D and E). RiskScore also showed a significant correlation with key immune-related signatures, including IFN-γ response, TGF-β response, and aneuploidy score, underscoring its impact on the tumor immune microenvironment (Figure 8F).

To assess potential chemotherapeutic responsiveness, we predicted drug sensitivity across risk groups using pRRophetic. Notably, BI-2536, GNF-2, WH-4-023, Vinorelbine, and A-443654 were predicted to be more effective in the high-risk group, while Roscovitine, HG-6-64-1, KIN001-135, Phenformin, and DMOG were more suitable for the low-risk group (Figure 9A). Finally, pathway analysis using ssGSEA revealed that RiskScore positively correlated with proliferation-related pathways (eg, E2F targets, G2M checkpoint), and negatively correlated with metabolism-related pathways (eg, bile acid metabolism, fatty acid metabolism) (Figure 9B). These findings suggest that the 9-lncRNA RiskScore not only reflects clinical aggressiveness and immune evasion, but also informs therapeutic stratification and targeted treatment decisions.

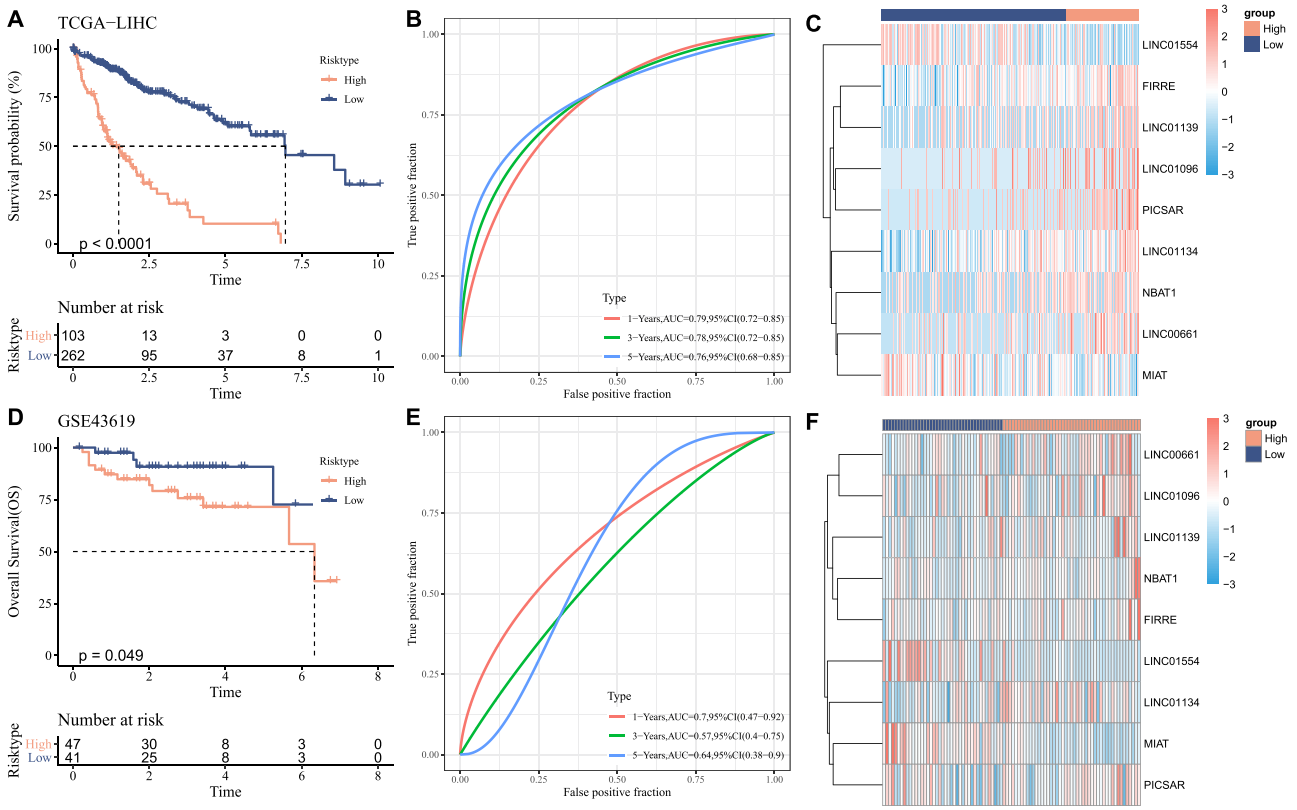

Figure 6 A prognostic risk model was constructed based on 9-lncRNA. (**A**–**C**) ROC curve of risk model, KM survival curve and heat map of 9-lncRNA expression between risk groups in TCGA cohort. (**D**–**F**) ROC curve of risk model, KM survival curve and 9-lncRNA expression heat map between risk groups in GSE43619 cohort.
Notes: (**A**, **D**) The X-axis represents the follow-up time (years), and the Y-axis indicates overall survival probability.

The Expression of Five lncRNAs Was Verified by RT-qPCR and Western Blotting

In order to verify the expression of five lncRNAs in the model, the liver cancer cell line Li-7 was inoculated into an ultra-low adsorption culture plate and cultured under hypoxia conditions for 24 hours to establish a hypoxia-anoikis model (Figure 10A). The expression of *LINC01554*, *FIRRE*, *LINC01139*, *LINC01134* and *NBAT1* was detected by RT-qPCR. The results showed that the expression of *LINC01554* decreased, while the expression of FIRRE, *LINC01139*, *LINC01134* and *NBAT1* was lower (Figure 10B). Subsequently, siRNA was employed to knock down the expression of *LINC01554* and *LINC01139* in Li-7 cells, with apoptosis evaluated under a hypoxia-anoikis model using flow cytometry. Compared to the control group, the expression levels of *LINC01554* and *LINC01139* were significantly reduced (Figure 10C). Notably, the proportion of apoptotic cells was decreased in the si-LINC01554 group and increased in the si-LINC01139 group relative to the si-NC group (Figure 10D).

Discussion

HCC is one of the leading causes of cancer-related deaths globally, with metastasis being a major contributor to patient mortality.[24] Due to the high rates of recurrence and metastasis, the prognosis for HCC patients after chemotherapy or drug treatment remains poor.[25] While some biomarkers assist in decision-making and guiding HCC treatment, they are still limited.[26] Alpha-fetoprotein (AFP) is an important diagnostic biomarker for HCC. However, over 30% of HCC patients exhibit AFP negativity, highlighting the critical need for new biomarkers.[27] LncRNAs, due to their tissue specificity, stability, and significant roles in gene regulatory networks, offer advantages as therapeutic and predictive biomarkers.[28] The *lncRNA MIR210HG* can promote HCC tumorigenesis and angiogenesis by upregulating the expression of mRNA *PFKFB4* and *SPAG4*, effectively predicting the prognosis of HCC patients. It can provide important clinical references for evaluating patient recurrence and metastasis risks.[29] The discovery and application of more lncRNA

https://doi.org/10.2147/JHC.S521878

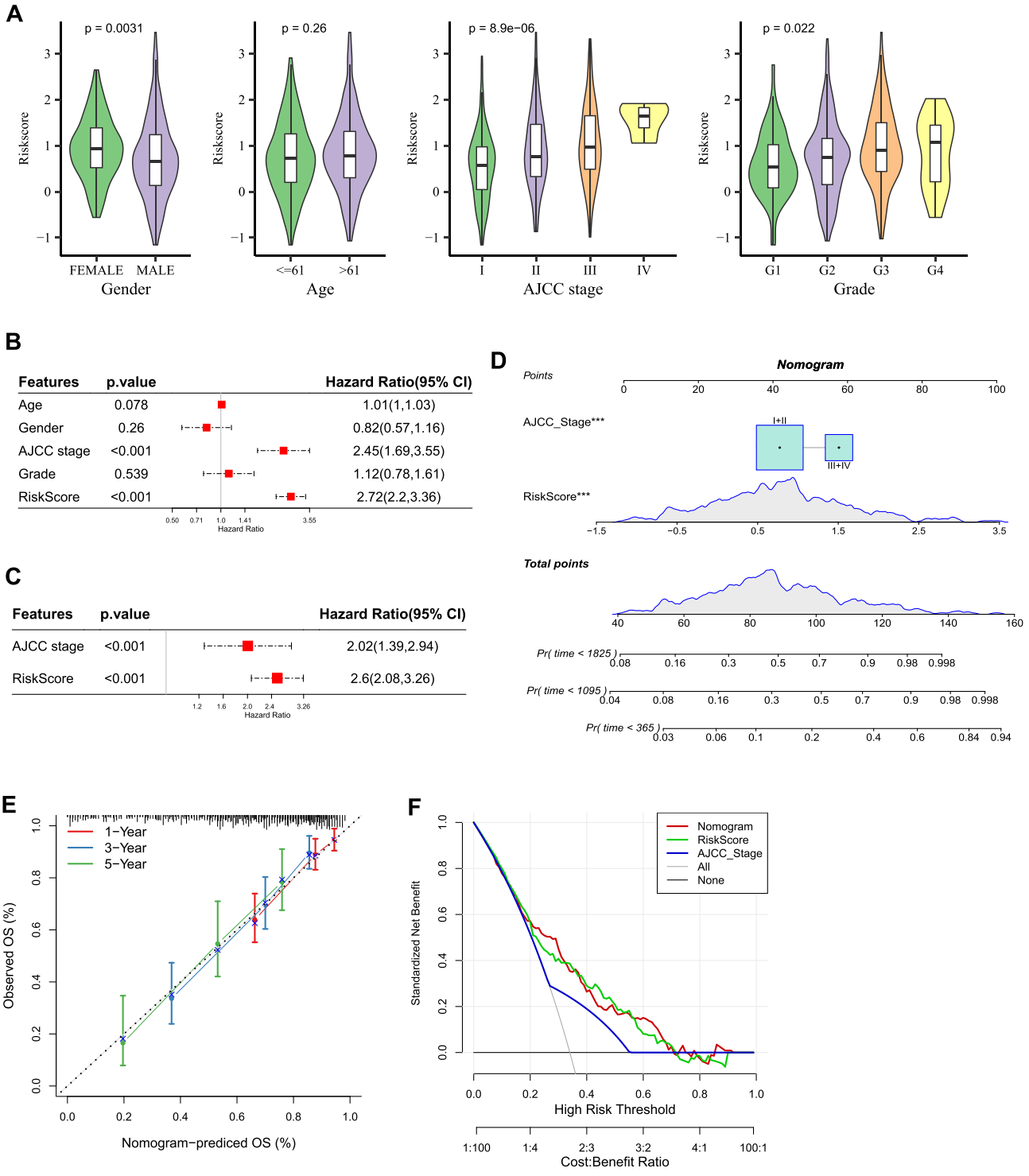

Figure 7 RiskScore combined with clinicopathological features to improve prognostic model and survival prediction. (**A**) Riskscore difference between clinical features in TCGA. (**B** and **C**) Riskscore and clinical characteristics of single factor and multivariate results. (**D**) Riskscore combined with AJCC Stage to establish a nomogram. (**E** and **F**) Calibration and Decision Curves for Nomogram.

biomarkers will significantly enhance the prediction and diagnostic capabilities of HCC metastasis, providing new avenues for developing personalized treatment strategies.

Hypoxia and anoikis are common stress factors in the tumor microenvironment that impact tumor progression and metastasis by regulating gene expression and cell signaling pathways. The hypoxia microenvironment induces significant

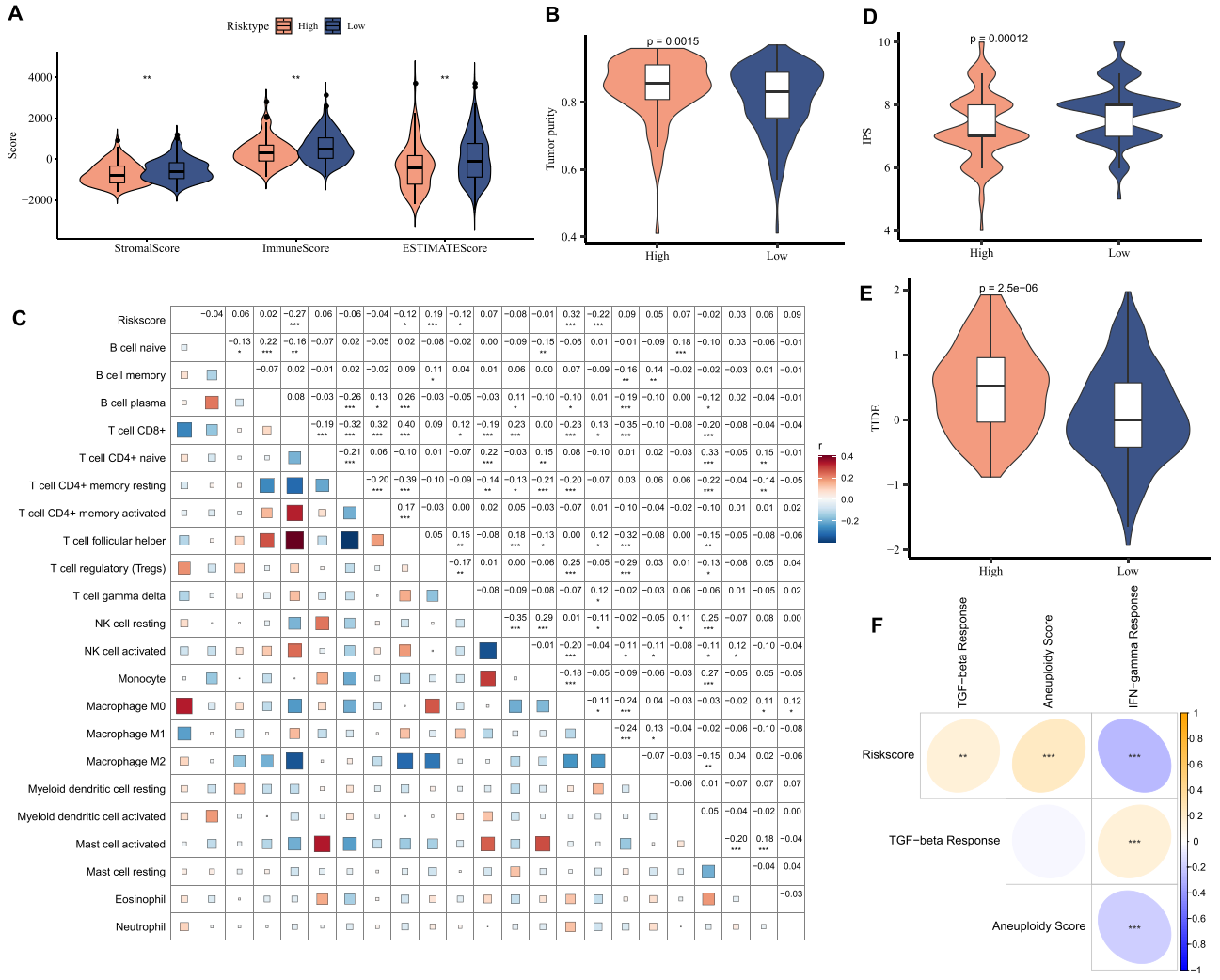

Figure 8 Difference analysis of tumor microenvironment in TCGA risk group. (**A**) ESTIMATE score between TCGA risk groups. (**B**) Tumor purity difference between TCGA risk groups. (**C**) Correlation between Riskscore and CIBERSOER immune score. (**D** and **E**) Comparison of immunotherapy sensitivity between TCGA risk groups. (**F**) Correlation analysis between Riskscore and IFN-gamma Response, TGF-beta Response, Aneuploidy score.
Notes: *p < 0.05, **p < 0.01, ***p < 0.001.

changes in the expression of numerous lncRNAs, impacting the behavior of HCC cells. *HABON* is transcriptionally activated by *HIF-1α* under hypoxia conditions to facilitate the transcriptional activation of *BNIP3*, leading to elevated *BNIP3* expression levels and promoting the growth, proliferation, and clone formation of HCC cells under hypoxia conditions.[30] Cancer recurrence and metastasis represent a multifaceted process involving various steps and factors, wherein evading anoikis serves as a pivotal stage.[31] HCC cells thwart anoikis and bolster metastasis through diverse molecular mechanisms, including integrin signaling, oxidative stress, and Epithelial-Mesenchymal Transition (EMT).[32–34] Notably, the collaboration between integrin β4 and the epidermal growth factor receptor (EGFR) enhances HCC resistance to anoikis by activating the FAK-AKT signaling pathway.[35] LncRNA plays a crucial role in the regulation of anoikis. For example, studies have shown that the *LncRNA FOXD2-AS1*/*miR7*/*TERT* pathway can enhance the survival rate and anchorage-independent growth of thyroid cancer cells.[36] *LncRNA HOTAIR* plays a crucial role in EMT by regulating the expression and activation of c-Met and its membrane co-localization partner Caveolin-1, as well as membrane organization, thereby helping HCC cells produce anoikis resistance and evade tumor immunity.[37] Our data indicate that certain lncRNAs undergo changes under hypoxia and anchorage-independent conditions, potentially serving as prognostic biomarkers for HCC.

https://doi.org/10.2147/JHC.S521878

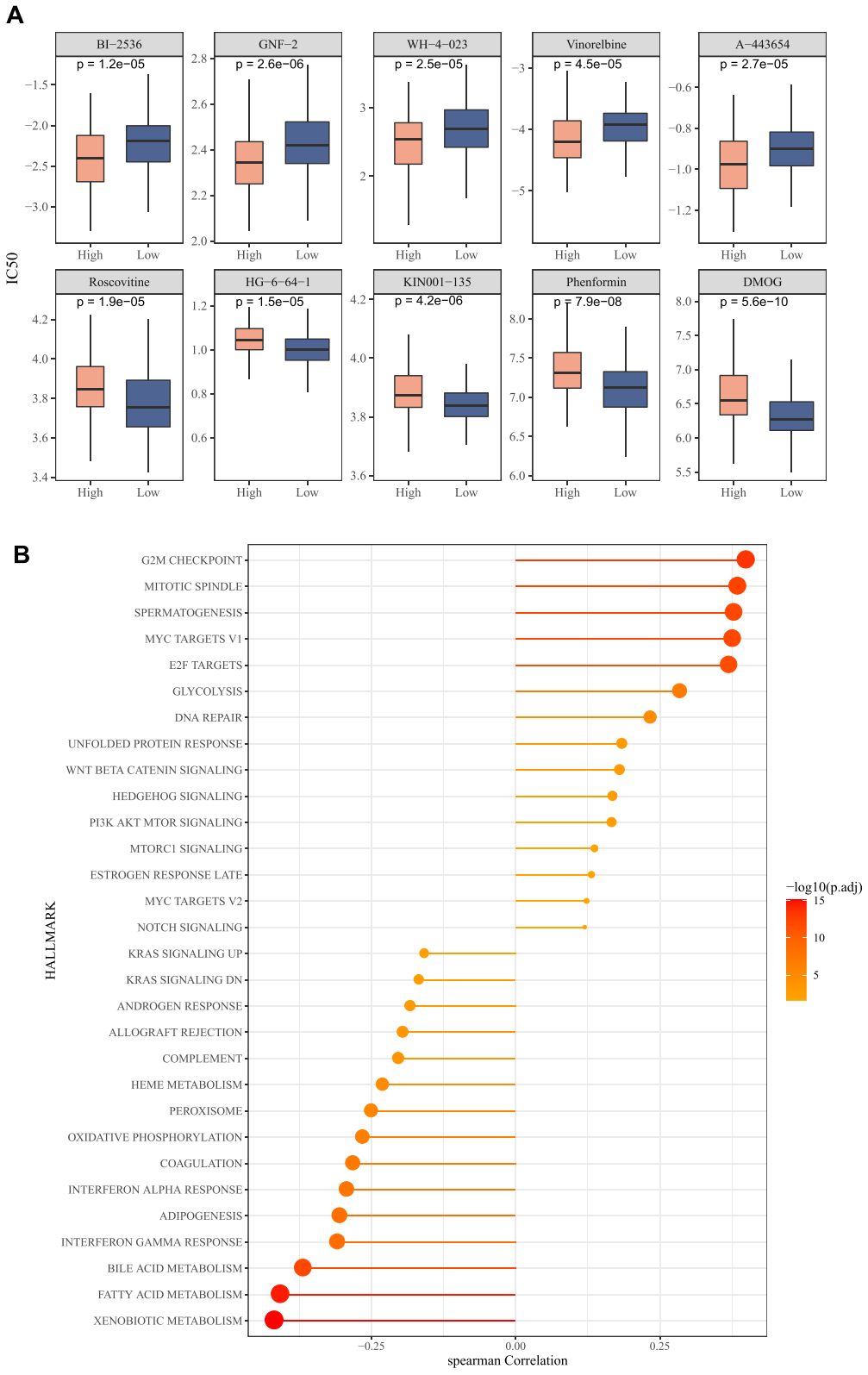

Figure 9 Drug sensitivity and functional enrichment analysis in the prognostic model. (**A**) Drug sensitivity difference between risk groups. (**B**) Riskscore and differential pathway correlation.

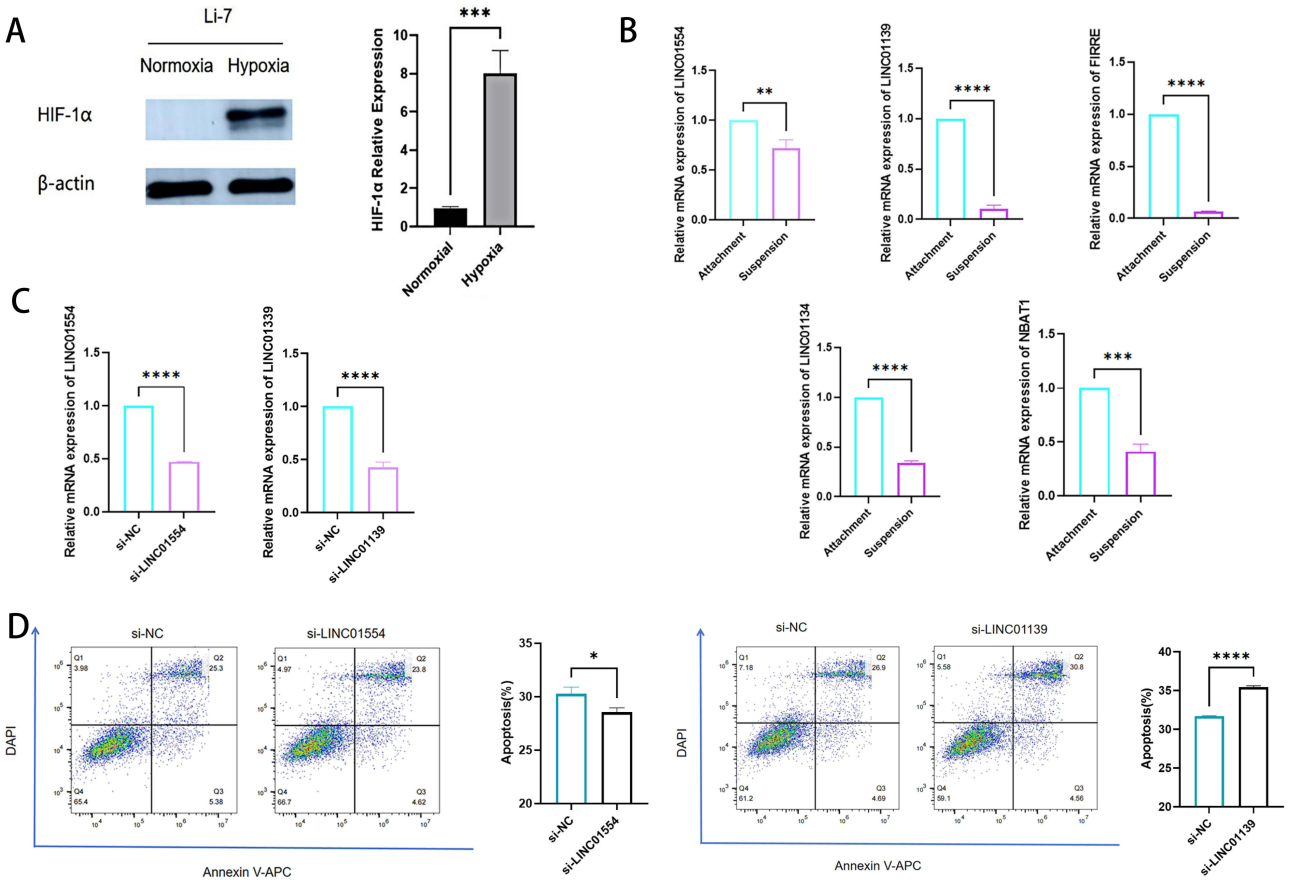

Figure 10 Western blotting and RT-qPCR were used to verify the LncRNA in the cell hypoxia and anoikis model. (**A**) Hypoxia of liver cancer cell line Li-7 was verified by Western blotting. (**B**) The relative expression of *LINC01554*, *FIRRE*, *LINC01139*, *LINC01134* and *NBAT1* mRNA. (**C**)The *LINC01554* and *LINC01139* interference efficiency in Li-7 cells was determined by RT-qPCR. (**D**) The percentage of apoptotic cells in si-LINC01554 and si-LINC01139 was determined by flow cytometry. The experimental data were expressed as the mean ± SD of the three independent experiments, and the asterisks indicated p values (** $p < 0.01$,*** $p < 0.001$,**** $p < 0.0001$).

In this study, through a comprehensive analysis of hypoxia- and anoikis-related lncRNAs, HCC patients were categorized into two molecular subtypes using cluster analysis. The proportion of subtype C1, characterized by a proliferative phenotype, and C2 immune subtypes exceeded that of subtype C2. HCC was classified into proliferative and non-proliferative subtypes, with the former displaying high proliferation rates, chromosomal instability, and activation of the Akt/mTOR signaling pathway.[38] The proliferative subtype correlated with immune subtypes C1 and C3, while C2 was linked to the non-proliferative subtype. Subtype C1 was distinguished by poor differentiation, elevated tumor grade, presence of macrovascular invasion, increased proliferation markers (*PLK1*, *MKI67*), and overexpression of stem cell genes (*EPCAM* and *AFP*).[39] This study revealed that tumor cells of C1 subtype tended to accumulate mutations, showcasing heightened heterogeneity and malignancy, resulting in a poorer patient prognosis. These findings suggest that the C1 subtype exhibits a stronger immune evasive capability and lower sensitivity to immunotherapy, whereas patients with the C2 subtype demonstrate a relatively improved prognosis.

Concerning immunotherapy, tumors are categorized into three types: immune-desert, immune-excluded, and immune-inflamed, determined by the presence and activity of immune cells within the tumor microenvironment.[40] Immune rejection primarily manifests as an immunosuppressive state, featuring ineffective immune cell infiltration that hinders T cells from reaching the core of the tumor due to various immunosuppressive factors.[41] The immune-inflamed type denotes an active immune response characterized by substantial infiltration of T cells and other immune cells in the tumor, alongside high expression levels of inflammation-related cytokines.[42] Our risk scoring model, based on nine lncRNAs, further confirmed the prognostic value of these lncRNAs in HCC. We noted that the high-risk group, particularly the C1 subtype, exhibited more immunosuppressive elements in the tumor microenvironment, including

increased expression of regulatory T cells (Tregs), inactivated M0 macrophages, and MDSC. This aligns with their lower responsiveness to immunotherapy, suggesting a potentially limited reaction to current immune checkpoint inhibitors (ICI). This corresponds to the characteristics of the "immune-excluded" subtype in HCC immunotyping, where tumors typically exhibit a highly immunosuppressive microenvironment that hinders immune cell infiltration and cytotoxic activity, and express high levels of immunosuppressive molecules such as PD-L1 and CTLA-4.[43] Notably, activated CD8+ T and NK cells coexist with immunosuppressive cells, suggesting a possible "immune-exhausted" state that may limit effector function.[44] This implies that immunosuppression could be a barrier to immunotherapy, highlighting the potential need for combined targeting strategies. Conversely, the low-risk group, primarily the C2 subtype, displayed reduced immunosuppressive factors and heightened immune cell activity, such as activated CD8+ T cells and memory CD4+ T cells, in line with the profiles of "immunoinflammatory" HCC. Immunoinflammatory HCC typically exhibits increased immune activity and enhanced sensitivity to ICI treatment. Consequently, patients with the C2 subtype show a more favorable prognosis and a more positive response to immunotherapy. Conversely, the high-risk group may demonstrate a diminished response to existing immune checkpoint inhibitors due to its specific traits. Potential therapeutic targets include PD-1/PD-L1, CTLA-4, TGF-β, and VEGF pathways, which, when targeted, can alleviate T cell suppression, improve the tumor microenvironment, and boost the anti-tumor immune response.[45] Different immunophenotypes of HCC display diverse responses to immune checkpoint inhibitors like PD-1/PD-L1 inhibitors, highlighting the need to explore combined treatment strategies to enhance outcomes.[46] For instance, the combination therapy of atezolizumab (anti-PD-L1) and bevacizumab (anti-VEGF) has received approval as a novel first-line treatment, significantly enhancing survival rates.[47] LncRNA holds substantial promise in immune combination therapy by regulating immune checkpoints, acting as a predictive biomarker, offering insights into therapeutic efficacy, and serving as a target or tool in combined therapy.[48–50] For example, *lncRNA UCA1* augments the anti-tumor effect of PD-1 inhibitors by suppressing miR-204-5p and boosting PD-L1 expression.[51] LncRNA can play a crucial role as a target or tool in collaboration with other treatments. As an illustration, si-PROX1-AS1 interacts with *miR-520d* to modulate PD-L1, promoting colorectal cancer (CRC) cell growth, spread, and evasion of the immune response.[52] These lncRNAs contribute to enhancing the effectiveness of immunotherapy and possess significant potential in combined immunotherapy.

In this study, a prognostic model was constructed based on nine hypoxia- and anoikis-related lncRNA (*LINC01554*, *MIAT*, *FIRRE*, *LINC01139*, *LINC01096*, *PICSAR*, *LINC01134*, *NBAT1*, *LINC00661*) genes, which revealed the important role of HCC in prognosis and tumor immunophenotype, as well as the metastasis and progression of HCC, and could be used as a reliable biomarker for predicting the prognosis and immunotherapy response of HCC. This study identifies hypoxia- and anoikis-related lncRNA subtypes and constructs a prognostic model, providing new insight into the molecular classification and treatment stratification of HCC.

Among the nine hypoxia- and anoikis-related lncRNAs, *LINC01554* and *LINC01139* were selected for focused experimental validation. Our results showed that under hypoxia and anoikis conditions, knockdown of *LINC01554* inhibited apoptosis, suggesting its role as a tumor suppressor. In contrast, knockdown of *LINC01139* significantly increased apoptosis, indicating that it promotes tumor cell survival. Previous studies have reported that *LINC01554* suppresses HCC progression by regulating the *miR-148b-3p*/*EIF4E3* axis, while *LINC01139* facilitates tumor development through the *miR-30*/*MYBL2* axis.[53,54] Moreover, *LINC01139* is involved in modulating glucose metabolism disturbances, remodeling the tumor microenvironment, and enhancing immunotherapy efficacy.[55] These lncRNAs may be regulated by the hypoxia-anoikis tumor microenvironment; however, their precise functions in HCC remain to be fully elucidated. The exact upstream regulatory mechanisms and downstream signaling pathways of these lncRNAs require further in-depth functional studies, representing important directions for future research.

Nonetheless, this study has several limitations. Although the prognostic value of our model was validated in both TCGA and GSE43619 cohorts, it has yet to be confirmed in larger, prospective, and multi-center clinical datasets to establish its true clinical utility. Moreover, while RT-qPCR was used to verify lncRNA expression, the precise mechanisms by which these lncRNAs regulate gene expression and cellular behavior remain unclear and require further functional investigation. Although preliminary apoptosis assays under hypoxia–anoikis conditions support their functional relevance, more comprehensive validations—including proliferation, migration, invasion assays, rescue

experiments, and exploration of downstream pathways such as PI3K/AKT and EMT—are necessary. Future studies should also integrate advanced techniques like single-cell sequencing and incorporate clinical samples to fully elucidate the roles of these lncRNAs in HCC progression and their potential clinical applications.

Ethical Statement

In accordance with Article 32 of the Ethical Review Measures for Life Sciences and Medical Research Involving Humans (China, 2023), secondary research using fully anonymized data in non-interventional settings is exempt from both ethical review and informed consent requirements. This study did not involve any interaction with human participants, collection of biological samples, or implementation of invasive procedures. Therefore, it meets the current regulatory criteria for exemption from institutional ethical approval and informed consent.

Acknowledgments

Special thanks to Guangxi Key Laboratory of Traditional Chinese Medicine and Preventive Medicine for supporting this study.

Disclosure

There is no conflict of interest in all authors.

References

1. Yang G, Yan H, Tang Y, et al. Advancements in understanding mechanisms of hepatocellular carcinoma radiosensitivity: a comprehensive review. *Chin J Cancer Res*. 2023;35(3):266–282.
2. Tamura S, Okamura Y, Sugiura T, et al. A comparison of the outcomes between surgical resection and proton beam therapy for single primary hepatocellular carcinoma. *Surg Today*. 2020;50(4):369–378. doi:10.1007/s00595-019-01888-5
3. Wu Z, Wang Z, Zhang L, et al. Updated results from ALTER-H004 trial: anlotinib combined with TACE as adjuvant therapy for patients with hepatocellular carcinoma at high risk of recurrence after surgery—A single arm, multi-center, phase II clinical trial. *J clin oncol*. 2023;41 (16_suppl):e16222–e16222. doi:10.1200/JCO.2023.41.16_suppl.e16222
4. Guo BJ, Ruan Y, Wang YJ, et al. Jiedu Recipe, a compound Chinese herbal medicine, inhibits cancer stemness in hepatocellular carcinoma via Wnt/β-catenin pathway under hypoxia. *J Integr Med*. 2023;21(5):474–486. doi:10.1016/j.joim.2023.06.008
5. Tarragó-Celada J, Cascante M. Targeting the metabolic adaptation of metastatic cancer. *Cancers*. 2021;13(7):1641. doi:10.3390/cancers13071641
6. Riaz F, Zhang J, Pan F. Forces at play: exploring factors affecting the cancer metastasis. *Front Immunol*. 2024;15:1274474. doi:10.3389/fimmu.2024.1274474
7. Wang Y, Li X, Shan J, Ding R, Cai J. Unraveling the role of anoikis in non-alcoholic fatty liver disease progression and immune cell infiltration. *Life Conflux*. 2025;1(2):e129. doi:10.71321/p63ws623
8. Husain A, Chiu YT, Sze KM, et al. Ephrin-A3/EphA2 axis regulates cellular metabolic plasticity to enhance cancer stemness in hypoxic hepatocellular carcinoma. *J Hepatol*. 2022;77(2):383–396. doi:10.1016/j.jhep.2022.02.018
9. Adeshakin FO, Adeshakin AO, Liu Z, et al. Upregulation of V-ATPase by STAT3 activation promotes anoikis resistance and tumor metastasis. *J Cancer*. 2021;12(16):4819–4829. doi:10.7150/jca.58670
10. Chen D, Yi R, Hong W, Wang K, Chen Y. Anoikis resistance of small airway epithelium is involved in the progression of chronic obstructive pulmonary disease. *Front Immunol*. 2023;14:1155478. doi:10.3389/fimmu.2023.1155478
11. Mai RY, Ye JZ, Gao X, et al. Up-regulated ITGB4 promotes hepatocellular carcinoma metastasis by activating hypoxia-mediated glycolysis and cancer-associated fibroblasts. *Eur J Pharmacol*. 2025;986:177102. doi:10.1016/j.ejphar.2024.177102
12. Luo Z, Luo Y, Xiao K. A-kinase interacting protein 1 promotes cell invasion and stemness via activating HIF-1α and β-catenin signaling pathways in gastric cancer under hypoxia condition. *Front Oncol*. 2022;11:798557. doi:10.3389/fonc.2021.798557
13. Wu J, Liu W, Qiu X, et al. A noninvasive approach to evaluate tumor immune microenvironment and predict outcomes in hepatocellular carcinoma. *Phenomics*. 2023;3(6):549–564. doi:10.1007/s43657-023-00136-8
14. Sharma U, Kaur Rana M, Singh K, Jain A. LINC00324 promotes cell proliferation and metastasis of esophageal squamous cell carcinoma through sponging miR-493-5p via MAPK signaling pathway. *Biochem Pharmacol*. 2023;207:115372. doi:10.1016/j.bcp.2022.115372
15. Huang Y, Zhang K, Li Y, Dai Y, Zhao H. The DLG1-AS1/miR-497/YAP1 axis regulates papillary thyroid cancer progression. *Aging*. 2020;12 (22):23326–23336. doi:10.18632/aging.104121
16. Li X, Du Y, Wang Y. The value of LncRNA SNHG5 as a marker for the diagnosis and prognosis of gastric cancer. *Am J Transl Res*. 2021;13 (5):5420–5427.
17. Yu H, Peng S, Chen X, Han S, Luo J. Long non-coding RNA NEAT1 serves as a novel biomarker for treatment response and survival profiles via microRNA-125a in multiple myeloma. *J Clin Lab Anal*. 2020;34(9):e23399. doi:10.1002/jcla.23399
18. Xie Y, Lin H, Wei W, et al. LINC00839 promotes malignancy of liver cancer via binding FMNL2 under hypoxia. *Sci Rep*. 2022;12(1):18757. doi:10.1038/s41598-022-16972-z
19. Zhou P, Lu Y, Zhang Y, Wang L. Construction of an immune-related six-lncRNA signature to predict the outcomes, immune cell infiltration, and immunotherapy response in patients with hepatocellular carcinoma. *Front Oncol*. 2021;11:661758. doi:10.3389/fonc.2021.661758

20. Tao H, Zhang Y, Yuan T, et al. Identification of an EMT-related lncRNA signature and LINC01116 as an immune-related oncogene in hepatocellular carcinoma. *Aging*. 2022;14(3):1473–1491. doi:10.18632/aging.203888
21. Zhu J, Zhao W, Yang J, Liu C, Wang Y, Zhao H. Anoikis-related lncRNA signature predicts prognosis and is associated with immune infiltration in hepatocellular carcinoma. *Anticancer Drugs*. 2024;35(5):466–480. doi:10.1097/CAD.0000000000001589
22. Charoentong P, Finotello F, Angelova M, et al. Pan-cancer immunogenomic analyses reveal genotype-immunophenotype relationships and predictors of response to checkpoint blockade. *Cell Rep*. 2017;18(1):248–262. doi:10.1016/j.celrep.2016.12.019
23. Thorsson V, Gibbs DL, Brown SD, et al. The immune landscape of cancer. *Immunity*. 2019;51(2):411–412. doi:10.1016/j.immuni.2019.08.004
24. Xie M, Lin Z, Ji X, et al. FGF19/FGFR4-mediated elevation of ETV4 facilitates hepatocellular carcinoma metastasis by upregulating PD-L1 and CCL2. *J Hepatol*. 2023;79(1):109–125. doi:10.1016/j.jhep.2023.02.036
25. Lu N, Min J, Peng L, et al. MiR-297 inhibits tumour progression of liver cancer by targeting PTBP3. *Cell Death Dis*. 2023;14(8):564. doi:10.1038/s41419-023-06097-0
26. Yang X, Yang C, Zhang S, et al. Precision treatment in advanced hepatocellular carcinoma. *Cancer Cell*. 2024;42(2):180–197. doi:10.1016/j.ccell.2024.01.007
27. Bian SX, Jia X, Zhang S, et al. P-143 Serum metabolomic identifies new diagnostic biomarkers for AFP-negative hepatocellular carcinoma. *Ann Oncol*. 2023;34:S65–S66. doi:10.1016/j.annonc.2023.04.199
28. Statello L, Guo CJ, Chen LL, Huarte M. Gene regulation by long non-coding RNAs and its biological functions. *Nat Rev Mol Cell Biol*. 2021;22(2):159. doi:10.1038/s41580-021-00330-4
29. Xie S, Zhong J, Zhang Z, et al. Novel risk model based on angiogenesis-related lncRNAs for prognosis prediction of hepatocellular carcinoma. *Cancer Cell Int*. 2023;23(1):159. doi:10.1186/s12935-023-02975-x
30. Ma CN, Wo LL, Wang DF, et al. Hypoxia activated long non-coding RNA HABON regulates the growth and proliferation of hepatocarcinoma cells by binding to and antagonizing HIF-1 alpha. *RNA Biol*. 2021;18(11):1791–1806. doi:10.1080/15476286.2020.1871215
31. Wang J, Luo Z, Lin L, et al. Anoikis-associated lung cancer metastasis: mechanisms and therapies. *Cancers*. 2022;14(19):4791. doi:10.3390/cancers14194791
32. Guha D, Saha T, Bose S, et al. Integrin-EGFR interaction regulates anoikis resistance in colon cancer cells. *Apoptosis*. 2019;24(11–12):958–971. doi:10.1007/s10495-019-01573-5
33. Díaz-Valdivia N, Simón L, Díaz J, et al. Mitochondrial dysfunction and the glycolytic switch induced by caveolin-1 phosphorylation promote cancer cell migration, invasion, and metastasis. *Cancers*. 2022;14(12):2862. doi:10.3390/cancers14122862
34. Ju S, Wang F, Wang Y, Ju S. CSN8 is a key regulator in hypoxia-induced epithelial-mesenchymal transition and dormancy of colorectal cancer cells. *Mol Cancer*. 2020;19(1):168. doi:10.1186/s12943-020-01285-4
35. Leng C, Zhang ZG, Chen WX, et al. An integrin beta4-EGFR unit promotes hepatocellular carcinoma lung metastases by enhancing Anchorage Independence through activation of FAK-AKT pathway. *Cancer Lett*. 2016;376(1):188–196. doi:10.1016/j.canlet.2016.03.023
36. Liu X, Fu Q, Li S, et al. LncRNA FOXD2-AS1 functions as a competing endogenous RNA to regulate TERT expression by sponging miR-7-5p in thyroid cancer. *Front Endocrinol*. 2019;10:207. doi:10.3389/fendo.2019.00207
37. Topel H, Bagirsakci E, Comez D, et al. lncRNA HOTAIR overexpression induced downregulation of c-Met signaling promotes hybrid epithelial/mesenchymal phenotype in hepatocellular carcinoma cells. *Cell Commun Signal*. 2020;18(1):110. doi:10.1186/s12964-020-00602-0
38. Chiang DY, Villanueva A, Hoshida Y, et al. Focal gains of VEGFA and molecular classification of hepatocellular carcinoma. *Cancer Res*. 2008;68(16):6779–6788. doi:10.1158/0008-5472.CAN-08-0742
39. Giraud J, Chalopin D, Blanc JF, Saleh M. Hepatocellular carcinoma immune landscape and the potential of immunotherapies. *Front Immunol*. 2021;12:655697. doi:10.3389/fimmu.2021.655697
40. Gerard CL, Delyon J, Wicky A, Homicsko K, Cuendet MA, Michielin O. Turning tumors from cold to inflamed to improve immunotherapy response. *Cancer Treat Rev*. 2021;101:102227. doi:10.1016/j.ctrv.2021.102227
41. Johnson A, Townsend M, O'Neill K. Tumor microenvironment immunosuppression: a roadblock to CAR T-cell advancement in solid tumors. *Cells*. 2022;11(22):3626. doi:10.3390/cells11223626
42. Binnewies M, Roberts EW, Kersten K, et al. Understanding the tumor immune microenvironment (TIME) for effective therapy. *Nat Med*. 2018;24(5):541–550. doi:10.1038/s41591-018-0014-x
43. Yang W, Liu S, Mao M, et al. T-cell infiltration and its regulatory mechanisms in cancers: insights at single-cell resolution. *J Exp Clin Cancer Res*. 2024;43(1):38. doi:10.1186/s13046-024-02960-w
44. Yi JS, Cox MA, Zajac AJ. T-cell exhaustion: characteristics, causes and conversion. *Immunology*. 2010;129(4):474–481. doi:10.1111/j.1365-2567.2010.03255.x
45. Bu MT, Chandrasekhar P, Ding L, Hugo W. The roles of TGF-β and VEGF pathways in the suppression of antitumor immunity in melanoma and other solid tumors. *Pharmacol Ther*. 2022;240:108211. doi:10.1016/j.pharmthera.2022.108211
46. Pinter M, Jain RK, Duda DG. The current landscape of immune checkpoint blockade in hepatocellular carcinoma: a review. *JAMA Oncol*. 2021;7(1):113–123. doi:10.1001/jamaoncol.2020.3381
47. Finn RS, Qin S, Ikeda M, et al. Atezolizumab plus bevacizumab in unresectable hepatocellular carcinoma. *N Engl J Med*. 2020;382(20):1894–1905. doi:10.1056/NEJMoa1915745
48. Peng L, Chen Z, Chen Y, Wang X, Tang N. MIR155HG is a prognostic biomarker and associated with immune infiltration and immune checkpoint molecules expression in multiple cancers. *Cancer Med*. 2019;8(17):7161–7173. doi:10.1002/cam4.2583
49. Arriaga-Canon C, Contreras-Espinosa L, Aguilar-Villanueva S, et al. The clinical utility of lncRNAs and their application as molecular biomarkers in breast cancer. *Int J Mol Sci*. 2023;24(8):7426. doi:10.3390/ijms24087426
50. Peng L, Chen Y, Ou Q, Wang X, Tang N. LncRNA MIAT correlates with immune infiltrates and drug reactions in hepatocellular carcinoma. *Int Immunopharmacol*. 2020;89(Pt A):107071. doi:10.1016/j.intimp.2020.107071
51. Wang X, Zhang Y, Zheng J, Yao C, Lu X. LncRNA UCA1 attenuated the killing effect of cytotoxic CD8 + T cells on anaplastic thyroid carcinoma via miR-148a/PD-L1 pathway. *Cancer Immunol Immunother*. 2021;70(8):2235–2245. doi:10.1007/s00262-020-02753-y
52. Li JS, Liu TM, Li L, Jiang C. LncRNA PROX1 antisense RNA 1 promotes PD-L1-mediated proliferation, metastasis, and immune escape in colorectal cancer by interacting with miR-520d. *Anticancer Drugs*. 2023;34(5):669–679. doi:10.1097/CAD.0000000000001437

53. Ren X, Wang X, Song H, et al. Long non-coding RNA LINC01554 overexpression suppresses viability, migration, and invasion of liver cancer cells through regulating miR-148b-3p/EIF4E3. *Heliyon*. 2024;10(6):e27319. doi:10.1016/j.heliyon.2024.e27319
54. Li ZB, Chu HT, Jia M, Li L. Long noncoding RNA LINC01139 promotes the progression of hepatocellular carcinoma by upregulating MYBL2 via competitively binding to miR-30 family. *Biochem Biophys Res Commun*. 2020;525(3):581–588. doi:10.1016/j.bbrc.2020.02.116
55. Gao Y, Yu J, Li Z, et al. Glucose metabolism perturbations influence tumor microenvironments via LINC01139 pathway and facilitate immunotherapy in hepatocellular carcinoma. *Genes Dis*. 2024;12(2):101302. doi:10.1016/j.gendis.2024.101302